Crashworthiness analysis of bioinspired thin-walled tubes based on Morpho wings microstructures

Hamid Nikkhah[1], Vincenzo Crupi[2*], Ahmad Baroutaji[3]

[1]Faculty of Engineering, School of Mechanical Engineering, University of Mohaghegh Ardabili, Ardabil, Iran

[2]Department of Engineering, University of Messina, Contrada di Dio, Sant' Agata, 98166 Messina, Italy

[3]School of Engineering, Faculty of Science and Engineering, University of Wolverhampton, Telford, UK

Abstract

Innovative structures, inspired by various biological microstructures in nature, have proved to be effective energy absorbing devices and showed extraordinary crashworthiness behavior. Thus, this paper presents a crashworthiness performance analysis of new thin-walled tubes bioinspired by the microstructure of Morpho wings. According to bio-inspiration concept, a total of 18 multi-layered tubes with different geometrical configurations were first developed. An experimentally validated finite element model was then constructed using LSDYNA and used to investigate the crush responses and deformation modes of the bio-inspired tubes. The key crashworthiness metrics including specific energy absorption (SEA), peak crush force (PCF), and crush force efficiency (CFE) were determined for the bioinspired structures and compared with the traditional structures. Furthermore, multi-criteria decision making method, known as Technique of Order Preference by Similarity to Ideal Solution (TOPSIS), was employed in order to identify the best crashworthiness design among the different proposed systems. It was found that the multi-layered bio-inspired tube with square cross sections and reinforcement walls outperformed all other designs and exhibited the best energy absorption capability.

Keywords:

Biomimetic; Bioinspired structures; Thin-walled tubes; Crashworthiness; Multi-Criteria Decision Making Method

---

*Corresponding author at: University of Messina, Contrada di Dio, Sant' Agata, 98166 Messina, Italy

E-mail address: crupi.vincenzo@unime.it

1. Introduction

Energy absorption structure is an essential part of any vehicle serving the purpose of absorbing the impact energy during a crush event and also reducing the injury risk of the occupants.

Thus, a significant amount of research has been conducted on the energy absorption capacity of thin walled structures, such honeycomb sandwich panels (Crupi et al. 2018; Palomba et al. 2018; Erdik 2020), aluminium fiber metal laminates (Sundaram et al. 2020) and thin walled tubes (Malekshahi et al. 2020; Magliaro and Altenhof 2020; Wierzbicki, and Abramowicz 1983).

Various solutions were suggested to improve the crashworthiness design of thin walled tubes: foam filled tubes (Li et al. 2020; Santosa et al. 2000; Sun et al. 2010), windowed tubes (Song et al. 2013), functionally - graded tubes (Li et al. 2015), multi-cell tubes (Fang et al. 2015), nested tubes (Baroutaji et al. 2016; Nikkhah et al. 2020; Tran et al. 2019), corrugated tubes (Mozafari et al. 2018). Baroutaji et al. (2017) summarized the recent developments related to thin-walled energy absorbers and their crashworthiness performance.

Innovative thin-walled tubes can be designed by based on biomimetic principles which seek to gain inspiration from nature for the development of new engineering solutions (Taylor 2015,

Genta 2016; Ha and Lu 2020). A comprehensive review on bio-inspired structures for energy absorption applications is provided by Ha and Lu (2020).

Different kinds of insects, such as Morpho butterflies and beetle, are well-known for their iridescence originating from nanostructures in the scales of their wings (Siddique et al. 2013). Such wings have different characteristics including a high degree of complexity, a variety of designs, light weight and high strength. The morpho wing was considered as an ideal model for biomimetic objects composed of lightweight functional materials (Kolle et al. 2010). These wings play a dual role of protecting the body and contributing to flight. Many researches have been done on insects' wings. Chen et al. (2015) reviewed the microstructure of the beetle's forewings and their associated features such as structural colours, and mechanical properties as well as their applications.

The goal of the current study is to apply the biomimetic approach in the design of thin walled structures for crashworthiness applications. Firstly, different bio-inspired thin walled tubes were proposed based on the morpho wings microstructure. Then, LSDYNA explicit finite element code was adopted to simulate the crush behavior of the structures. The results of the FE model were compared against experimental measurements and excellent prediction capability was revealed by the developed model. Following the validation of the FE model, the crush behavior and energy absorption capability of the bio-inspired tubes were explored and compared. Finally, the best bio-inspired design was determined using TOPSIS multi-criteria decision making method.

2. Materials and methods

2.1. Geometry and material of *Morpho bio-inspired tubes*

As mentioned earlier, the designs presented in this paper were bio-inspired by the microstructure of the Morpho butterfly wings. The Morpho wing, as shown in Fig. 1, has a complex and sophisticated structure where it is composed of a wing base termed as 'lamellae' surrounded by an multilayer system of chitin known as 'ridges' (Siddique et al. 2013; Kolle et al. 2010). Such hierarchical and complex structure is responsible for providing the unique optical, lightweight, and mechanical properties of the morpho wings which allow them to serve a number of functions, including active and stable flying, interacting with light and sound production (Tippets et al. 2016; Zhang et al. 2014). Such properties show the potential to biomimetic the microstructure of morpho wings for creating lightweight crashworthiness designs.

Based on the hierarchical structure of the ridges in the morpho wings, as shown in Fig1.c, a total of 18 designs were proposed in this paper. The bio-inspired structures are consisted of three thin-walled tubes with different geometrical shapes stacked vertically together in layers format. Circular, square, or hexagonal tubes were used to form the different layers of the structures. All the tubes featured the same cross-sectional area of 900 mm^2, a wall thickness of 1.8 mm, and a width of 20 mm. These tubes were arranged together either by directly placing them over each other or by using vertical webs with a length of 20 mm among the layers. The various geometrical configurations of the multi-layer bio-inspired tubes with and without vertical webs are shown in Fig. 2.

Carbon steel, prepared according to DIN 17100 ST 37.3 standard and contains around 0.19% C and 1.7% Mn, was used to manufacture the different samples in this study. Three standard tensile tests were carried out using universal test machine (SANTAM-40) to evaluate the

mechanical behavior of this steel. As a result of the tensile tests, the true stress-strain curve was obtained as presented in Fig. 3. This stress strain curve was used to obtain the key mechanical properties of the material required for the FE modelling in the subsequent section.

2.2. Finite element modelling

The energy absorbing capability of the Morpho wings was analyzed using the nonlinear finite element code LS-DYNA. The finite element model, as shown in Fig 4, is consisted of three main parts including the upper moving base, the bio-inspired structure, and the lower base plate. The upper base is modelled as a rigid wall and constrained to travel only along the Z direction. This rigid wall has a mass of 800 kg and moves at a velocity of 20 m/s to impact the structure at its top end. The mass was chosen to ensure sufficient deformation of the tube upon impact while the travelling speed is a typical value used for the automobile crashworthiness applications (Nagel and Thambiratnam. 2006). The base was also modeled as a rigid body and constrained not to move or rotate in any direction.

The piecewise-linear-plasticity model of LS-DYNA was considered for modeling the material behavior of the bio-inspired tube. The material model featured a bulk material density of 7860 kg/m^3, Young's modulus of 200 GPa, Poisson's ratio of 0.3, yield stress of 248 MPa, and ultimate tensile stress of 407 MPa. These properties were obtained from the true stress-strain curve shown in Fig. 3. The structures were meshed using Belytschko-Tsay 4-node shell element with five integration points through the thickness as it is suitable for capturing the large deformation effects of thin-walled tubes under the impact loading (Nikkhah et al. 2017). Mesh convergence analysis was conducted to determine the mesh element size. It was found that the optimal mesh size for the tubes is 1 mm which allows convergence of the solution within a

reasonable computing time. An automatic surface to surface contact was used to define the contacts between the tubes and the rigid bodies. Meanwhile, an automatic single surface contact type was employed to represent the self-contact of the tubes during the plastic deformation. A friction coefficient of 0.2 was assigned for all contact pairs in the model.

2.3.Experimental tests

With the aim of validating the FE model developed and described in the previous section, quasi-static experimental crush tests were executed on traditional and bio-inspired samples using SANTAM STM-50 test machine. The tested samples included traditional tubes with circular, hexagonal, and square geometry as well as multi-layered tube with H-C-S configuration. The geometries of the tested tubes are shown in the Fig 5. All the tested samples were prepared using wire-cut electric discharge machine (WEDM).

Each crushing test was conducted under displacement control settings where the upper crosshead of SANTAM STM-50 test machine was displaced downward at a predefined velocity of 10 mm/min until crushing more than 60% of the total length of the sample. The lateral load was recorded via the machine loading cell while the displacement was determined by measuring the crosshead movement and thus the load -displacement curves of the crush tests were obtained.

2.4.Crashworthiness parameters

In order to quantitatively evaluate the crashworthiness performance, and consequently to determine the best crashworthiness bio-inspired design, the following three important crashworthiness indicators were calculated and compared: specific energy absorption (SEA), peak crush force (PCF) and crush force efficiency (CFE) (Baroutaji et al. 2016).

The specific energy absorption (SEA) is the energy absorption (EA) divided by the density (ρ) of the tube and it can be calculated as shown in Eq. 1 (Palomba et al. 2018):

$$SEA = \frac{EA}{\rho} = \frac{\int_0^d F(x)\,dx}{\rho} \quad (1)$$

Where F(x) and d are the instantaneous load and the deformation distance, respectively. As a general rule, the greater the SEA, the better the energy absorption behavior.

Peak crush force (PCF) is defined as the highest force magnitude observed in the force-displacement response. Generally, a lower PCF is preferred to prevent instant deceleration which is undesirable for crashworthiness. So conversely to SEA, the lower the PCF, the better the energy absorption structure.

Consequently, crush force efficiency (CFE) can be expressed using Eq. (2):

$$CFE = \frac{MCF}{PCF} \times 100\% \quad (2)$$

where MCF is the mean crushing force. For the crashworthiness design, the higher the CFE, the better the consistency in energy absorption throughout the collapse spectrum.

2.5. TOPSIS multi-criteria decision making method

Technique of Order Preference by Similarity to Ideal Solution (TOPSIS), which is a multi-criteria decision making method (Lei et al. 2020), was used to determine the best bio-inspired configuration among the different designs proposed in this paper. This method was developed by Hwang and Yoon (1981) and it was fully explained in authors' previous work (Nikkhah et al. 2019; Nikkhah et al. 2020). TOPSIS considered 18 alternatives representing the number of the bio-inspired tubes in this study and 54 design criteria representing the crashworthiness metrics of

the tubes including 18×SEA, 18×PCF, and 18×CFE. Two artificial ideal alternatives were assumed within the framework of TOPSIS. The positive ideal alternative is the design which has the best level for all indices. Meanwhile, the negative ideal alternative is the design which has the worst indices. TOPSIS seeks for the alternative that is closest to the positive ideal solution and farthest from the negative ideal alternative.

3. Results and discussion

3.1 Validation of the numerical model

Fig 6 compares the numerical and experimental crush responses in terms of load-displacement curves and deformation modes for all tested samples including traditional and bioinspired ones. It is clear that the simulation results are in satisfactory agreement with the experimental ones. Only two shortcomings can be observed in the predictions capability of the FE models. The FE model of the circular tube overestimates the crush force at the final stages of deformation while an underestimation of crush force is offered by the FE model of the H-C-S tube at the early stages of deformation. However, such shortcomings didn't have major consequences on the ability of the FE models to simulate the deformation modes and it is clear that the deformed profiles of all tested samples are well captured by the numerical models. Table1 shows the crashworthiness metrics as obtained from tests and simulations for all tested samples. It is clear that all numerical models are able of predicting the crashworthiness metrics accurately. Thus, the finite element models were considered to be sufficiently accurate and can be used to investigate the crashworthiness responses of the other bio-inspired structures and to undertake further comparative analysis.

3.2 Crashworthiness analysis of Morpho inspired thin-walled tubes

The crush responses and the final deformation profiles of the bio-inspired tubes with reinforcement walls are shown in Fig 7. For the structures with the square tube in the top layer including S-S-S, S-C-H, and S-H-C, the crush force initially increased steeply to its peak value then decreased suddenly and subsequently fluctuated for the remaining of the crushing stroke. Such behavior could be due to the fact that the square tube is the first to be deformed upon impact in these structures and thus its crushing pattern, characterized by initial peak force as shown previously in Fig 6.b, dominates the force-displacement response of these structures during the early stages of the deformation process. For the rest of tubes, the post-collapse stage showed an almost flat response where the crushing force was constant during the crushing process. Interestingly, for all tubes in this group, i.e. tubes with reinforcement walls, the vertical webs didn't deform significantly and they basically acted more or less as triggers to deform the tubes in the middle and lower layers.

The force-displacement curves and deformation modes of the simple and layered structures without reinforcement walls are shown in Fig 8. The crush responses of the traditional tubes were only presented for comparison purposes. The crush responses of the traditional tubes were only presented for comparison purposes. The bio-inspired tubes without the reinforcement walls exhibited irregular crush responses in which peak crush forces appeared at the final stages of the deformation process due to structure self-contact and material densification. Such behavior was not observed in the tubes with vertical webs and this indicates that the vertical webs play a key role in creating a more stable crushing response.

In general, the collapse mode of a thin-walled tube under lateral loading is plastic bending at the locations of the plastic hinges. Such collapse behavior can be seen for both groups of bio-

inspired structures and the traditional tubes. For the tubes with vertical webs, additional plastic hinges were created at the connection points between the webs and the tubes and this led to higher energy absorption capacity of these tubes.

The crashworthiness metrics of all traditional and bio-inspired tubes including SEA, PCF, and CFE are presented in Fig. 9. As can be seen, the traditional tubes absorb the lowest SEA among all the studied structures. This is basically due to the fact that the lateral deformation of the traditional tubes yields very limited plastic zones and thus only a small volume of the tube's material absorbs energy. However, the traditional tubes seem to exhibit a better CFE response than that of the bio-inspired structures without the vertical webs. Such trend can be attributed to the stable force-displacement responses offered by the traditional tubes. For the bio-inspired tubes, it is clear that the tubes with the vertical reinforcement walls exhibit higher SEA, higher CFE, and lower PCF than their counterparts without reinforcement walls. Also, it is clear that the structures with the square tube in the top layer, such as S-S-S, S-C-H, S-H-C, absorbed more energy than other configurations. However, these tubes have also shown higher PCF and lower CFE.

3.3 Identifying the best configuration using TOPSIS method

In this study, the TOPSIS is employed to determine the best energy absorber using the crashworthiness responses of SEA, PCF, and CFE as presented in Table 2.

Considering that the good crashworthiness performance is characterized by high SEA, high CFE, and low PCF, SEA and CFE were considered as the beneficial index whereas PCF was considered as the non-beneficial index (Lei et al. 2020). Same weighting was assigned for beneficial and non- beneficial indices. Based on TOPSIS, the tubes were ranked from 1 to 18

where 1 is the best and 18 is the worst energy absorber as shown in Table 1. From the TOPSIS analysis, it can be seen that the highest and lowest scores were obtained by S-S-S and H-C-S tubes, respectively. Thus, S-S-S tube was deemed to be the best bio-inspired structure as determined by TOPSIS method.

4. Conclusion

This paper proposes new thin-walled tubes inspired by Morpho wings microstructure for crashworthiness applications. Based on the multi-layer pattern observed in the ridges microstructure of Morpho wings, two groups of multi-layered structures were considered; first with vertical webs between the different layers of the structure; and the second without these webs. Using LS-DYNA, numerical models were created for the traditional and bio-inspired structures where their crushing responses were validated using experimental tests. The crashworthiness performance of the traditional and bio-inspired tubes was assessed via various metrics including SEA, PCF, and CFE. Additionally, the TOPSIS method was used to determine the best design. The bio-inspired structures with vertical webs were found to outperform their counterparts without vertical webs. However, the vertical webs themselves were not deformed during the crushing process but they have triggered extra plastic hinges in the structure leading to greater energy dissipation. Based on the TOPSIS, S-S-S structure which features square tubes across the three layers was found to be the best structure among the 18 designs studied in this paper. S-S-S tube offered 75% and 50% higher SEA than its counterparts with circular and hexagonal tubes, i.e. C-C-C and H-H-H, respectively. The bio-inspiration methodology adopted in this study proved to be beneficial for developing effective structures for energy absorption and crashworthiness applications.

5. References

Baroutaji, A., M.D. Gilchrist, and A.G. Olabi. 2016. Quasi-Static, Impact and Energy Absorption of Internally Nested Tubes Subjected to Lateral Loading. *Thin-Walled Structures* 98: 337–50. doi: 10.1016/j.tws.2015.10.001.

Baroutaji, A., M. Sajjia, and A.G. Olabi. 2017. On the Crashworthiness Performance of Thin-Walled Energy Absorbers: Recent Advances and Future Developments. *Thin-Walled Structures* 118: 137–63. doi: 10.1016/j.tws.2017.05.018.

Chen, J., J. Xie, Z. Wu, E. M. A. Elbashiry, and Y. Lu. 2015. Review of Beetle Forewing Structures and Their Biomimetic Applications in China: (I) on the Structural Colors and the Vertical and Horizontal Cross-Sectional Structures. *Materials Science and Engineering C* 55: 605-619. doi: 10.1016/j.msec.2015.05.064.

Crupi, V., E. Kara, G. Epasto, E. Guglielmino, and H. Aykul. 2018. Theoretical and Experimental Analysis for the Impact Response of Glass Fibre Reinforced Aluminium Honeycomb Sandwiches. *Journal of Sandwich Structures & Materials* 20 (1): 42–69. doi: 10.1177/1099636216629375.

Erdik, A. 2020. Experimental and Numerical Study on Dynamic Response of V-Shaped Hull Subjected to Mine Blast. *Mechanics Based Design of Structures and Machines*. Advance online publication. doi: 10.1080/15397734.2020.1726775.

Fang, J., Y. Gao, G. Sun, N. Qiu, and Q. Li. 2015. On Design of Multi-Cell Tubes under Axial and Oblique Impact Loads. *Thin-Walled Structures* 95: 115–26. doi:

10.1016/j.tws.2015.07.002.

Genta, G. 2016. Are There Severe Limitations to the Bioinspired Approach in Machine Design? *Proceedings of the Institution of Mechanical Engineers, Part C: Journal of Mechanical Engineering Science* 230 (9): 1511–20. doi: 10.1177/0954406215576064.

Ha, N. S., and G. Lu. 2020. A Review of Recent Research on Bio-Inspired Structures and Materials for Energy Absorption Applications. *Composites Part B: Engineering* 181: 107496 doi: 10.1016/j.compositesb.2019.107496.

Hwang, C.-L., and K. Yoon. 1981. Methods for Multiple Attribute Decision Making. In: Multiple Attribute Decision Making. Lecture Notes in Economics and Mathematical Systems, 186: 58–191. Springer, Berlin, Heidelberg. doi: 10.1007/978-3-642-48318-9_3

Kolle, M., P. Salgard-Cunha, M. Scherer, F. Huang, P. Vukusic, S. Mahajan, J. J. Baumberg, and U. Steiner. 2010. Mimicking the Colourful Wing Scale Structure of the Papilio Blumei Butterfly. *Nature Nanotechnology* 5 (7): 511–515. doi: 10.1038/nnano.2010.101.

Lei, F., X. Lv, J. Fang, G. Sun, and Q. Li. 2020. Multiobjective Discrete Optimization Using the TOPSIS and Entropy Method for Protection of Pedestrian Lower Extremity. *Thin-Walled Structures* 152: 106349. doi: 10.1016/j.tws.2019.106349.

Li, G., Z. Zhang, G. Sun, X. Huang, and Q. Li. 2015. Comparison of Functionally-Graded Structures under Multiple Loading Angles. *Thin-Walled Structures* 94: 334–347. doi: 10.1016/j.tws.2015.04.030.

Li, S., X. Guo, J. Liao, Q. Li, and G. Sun. 2020. Crushing Analysis and Design Optimization for Foam-Filled Aluminum/CFRP Hybrid Tube against Transverse Impact. *Composites Part B:*

Engineering 196: 108029. doi: 10.1016/j.compositesb.2020.108029.

Magliaro, J., and W. Altenhof. 2020. Energy Absorption Mechanisms and Capabilities for Magnesium Extrusions under Impact. *International Journal of Mechanical Sciences* 179: 105667. doi: 10.1016/j.ijmecsci.2020.105667.

Malekshahi, A., M. Hosseini, and A. N. M. Ansari. 2020. Theoretical Estimation of Axial Crushing Behavior of Multicell Hollow Sections. *Mechanics Based Design of Structures and Machines*. Advance online publication. doi: 10.1080/15397734.2020.1776133.

Mozafari, H., A. Eyvazian, A. M. Hamoud, V. Crupi, G. Epasto, E. Gugliemino. 2018. Numerical and experimental investigation of corrugated tubes under lateral compression. *International Journal of Crashworthiness* 23(4): 461-473 doi: 10.1080/13588265.2017.1345592.

Nagel, G.M. and D.P. Thambiratnam. 2006. Dynamic simulation and energy absorption of tapered thin-walled tubes under oblique impact loading. *International Journal of Impact Engineering* 32(10): 1595–1620 doi: 10.1016/j.ijimpeng.2005.01.002.

Nikkhah, H., A. Baroutaji, Z. Kazancı, and A. Arjunan. 2020. Evaluation of Crushing and Energy Absorption Characteristics of Bio-Inspired Nested Structures. *Thin-Walled Structures* 148: 106615 doi: 10.1016/j.tws.2020.106615.

Nikkhah, H., A. Baroutaji, and A. G. Olabi. 2019. Crashworthiness Design and Optimisation of Windowed Tubes under Axial Impact Loading. *Thin-Walled Structures* 142: 132–48. doi: 10.1016/J.TWS.2019.04.052.

Nikkhah, H., F. Guo, Y. Chew, J. Bai, J. Song, and P. Wang. 2017. The Effect of Different

Shapes of Holes on the Crushing Characteristics of Aluminum Square Windowed Tubes under Dynamic Axial Loading. *Thin-Walled Structures* 119: 412–20. doi: 10.1016/j.tws.2017.06.036.

Palomba, G., G. Epasto, V. Crupi, and E. Guglielmino. 2018. Single and Double-Layer Honeycomb Sandwich Panels under Impact Loading. *International Journal of Impact Engineering* 121: 77–90. doi: 10.1016/j.ijimpeng.2018.07.013.

Potyrailo, R. A., R. K. Bonam, J. G. Hartley, T. A. Starkey, P. Vukusic, M. Vasudev, T. Bunning, et al. 2015. Towards Outperforming Conventional Sensor Arrays with Fabricated Individual Photonic Vapour Sensors Inspired by Morpho Butterflies. *Nature Communications* 6 (1): 1–12. doi: 10.1038/ncomms8959.

Santosa, S. P., T. Wierzbicki, A. G Hanssen, and M. Langseth. 2000. Experimental and Numerical Studies of Foam-Filled Sections. *International Journal of Impact Engineering* 24 (5): 509–34. doi: 10.1016/S0734-743X(99)00036-6.

Siddique, R. Hasan, S. Diewald, J. Leuthold, and H. Hölscher. 2013. Theoretical and Experimental Analysis of the Structural Pattern Responsible for the Iridescence of Morpho Butterflies. *Optics Express* 21 (12): 14351. doi: 10.1364/oe.21.014351.

Song, J., Y. Chen, and G. Lu. 2013. Light-Weight Thin-Walled Structures with Patterned Windows under Axial Crushing. *Internatonal Journal of Mechanical Sciences* 66: 239–48. doi: 10.1016/j.ijmecsci.2012.11.014.

Sun, G., G. Li, S. Hou, S. Zhou, W. Li, and Q. Li. 2010. Crashworthiness Design for Functionally Graded Foam-Filled Thin-Walled Structures. *Materials Science and*

Engineering: A 527: 1911–19. doi: 10.1016/j.msea.2009.11.022.

Sundaram, S. K., A. G. Bharath, and B. Aravind. 2020. Influence of Target Dynamics and Number of Impacts on Ballistic Performance of 6061-T6 and 7075-T6 Aluminum Alloy Targets. *Mechanics Based Design of Structures and Machines*. Advance online publication. doi: 10.1080/15397734.2020.1738245.

Taylor, D. 2015. Fatigue-resistant components: What can we learn from nature? *Proceedings of the Institution of Mechanical Engineers, Part C: Journal of Mechanical Engineering Science* 229 (7): 1186–1193 doi: 10.1177/0954406214530881.

Tippets, C. A., Y. Fu, A. M. Jackson, E. U. Donev, and R. Lopez. 2016. Reproduction and Optical Analysis of Morpho-Inspired Polymeric Nanostructures. *Journal of Optics* 18 (6): 065105. doi: 10.1088/2040-8978/18/6/065105.

Tran, T. N., D. H. Le, and A. Baroutaji. 2019. Theoretical and Numerical Crush Analysis of Multi-Stage Nested Aluminium Alloy Tubular Structures under Axial Impact Loading. *Engineering Structures* 182: 39–50. doi: 10.1016/j.engstruct.2018.12.072.

Wierzbicki, T., and W. Abramowicz. 1983. On the Crushing Mechanics of Thin-Walled Structures. *Journal of Applied Mechanics* 50 (4a): 727–34. doi: 10.1115/1.3167137.

Zhang, W., J. Gu, Q. Liu, H. Su, T. Fan, and D. Zhang. 2014. Butterfly Effects: Novel Functional Materials Inspired from the Wings Scales. *Physical Chemistry Chemical Physics* 16 (37): 19767–80. doi: 10.1039/c4cp01513d.

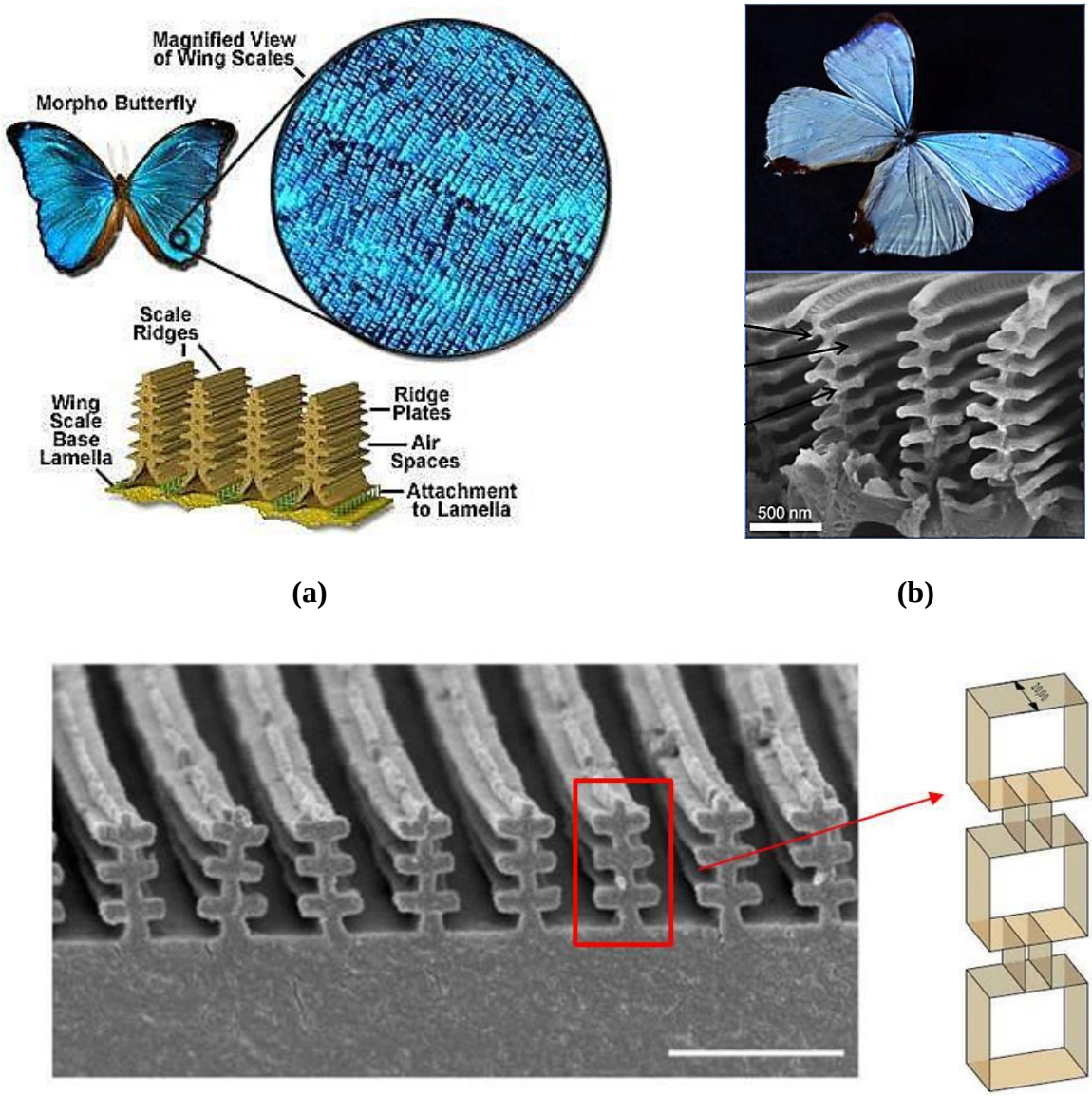

Fig. 1 The Morpho Butterfly microstructure adapted from (Potyrailo et al. 2015), (a) the macro-structure of the wings, (b) microstructure showing Lamellae in Ridges that forms the wings architecture, (c) The cross-section of morpho wings periodic microstructures (Tippets et al. 2016).

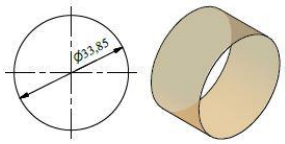

C

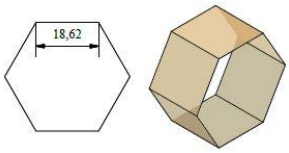

H

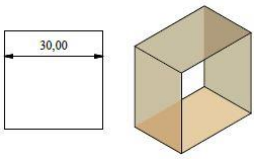

S

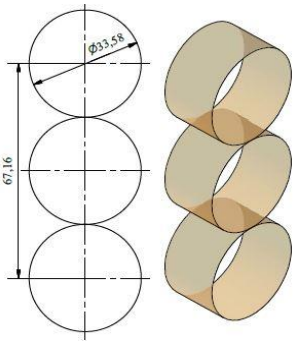

CCC

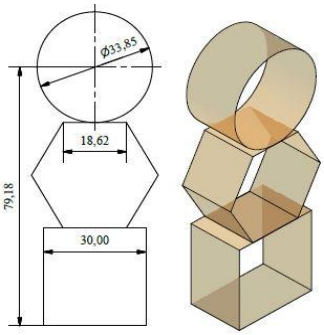

CHS

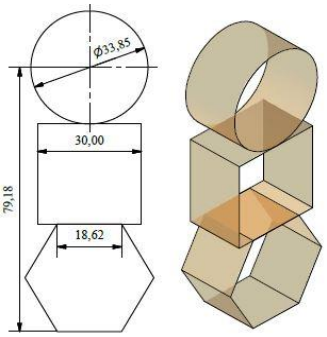

CSH

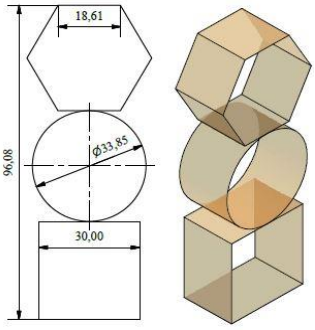

HCS

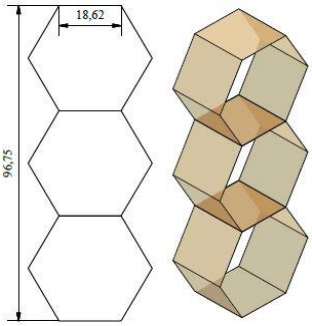

HHH

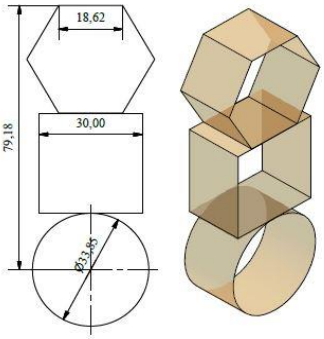

HSC

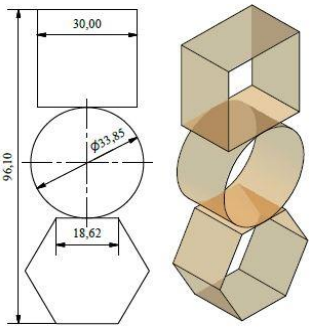

SCH

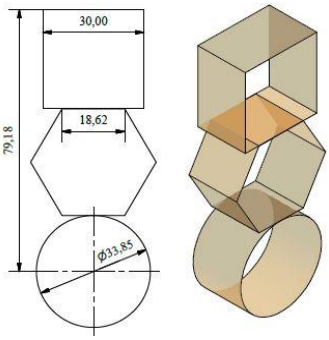

SHC

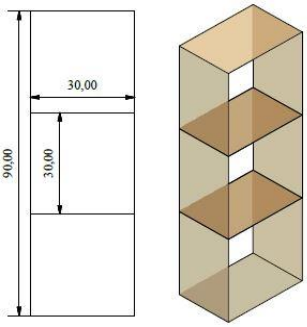

SSS

(a)

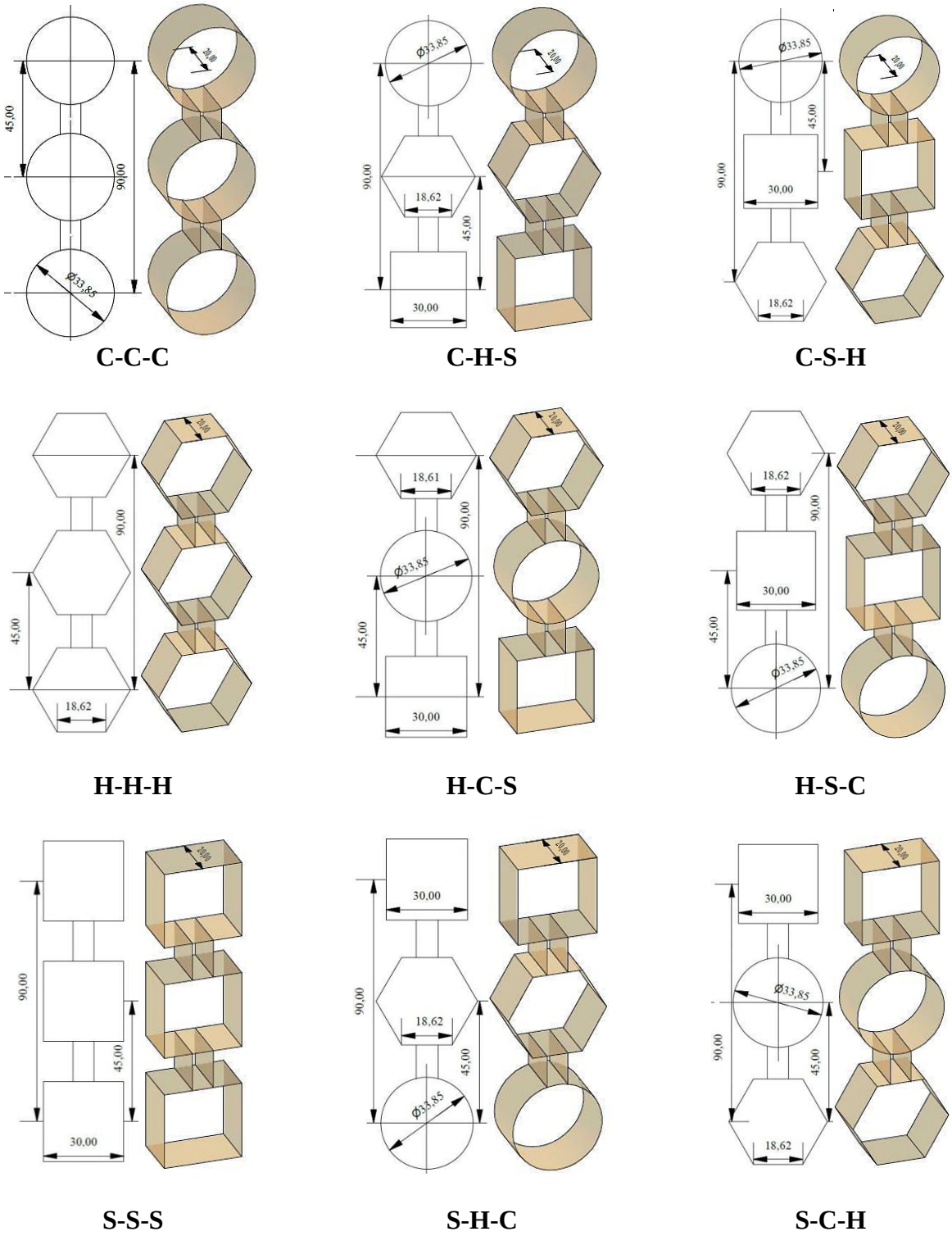

(b)

Fig. 2 Geometry specifications of the bioinspired tubes: a) without reinforcement walls, b) with reinforcement walls hexagonal

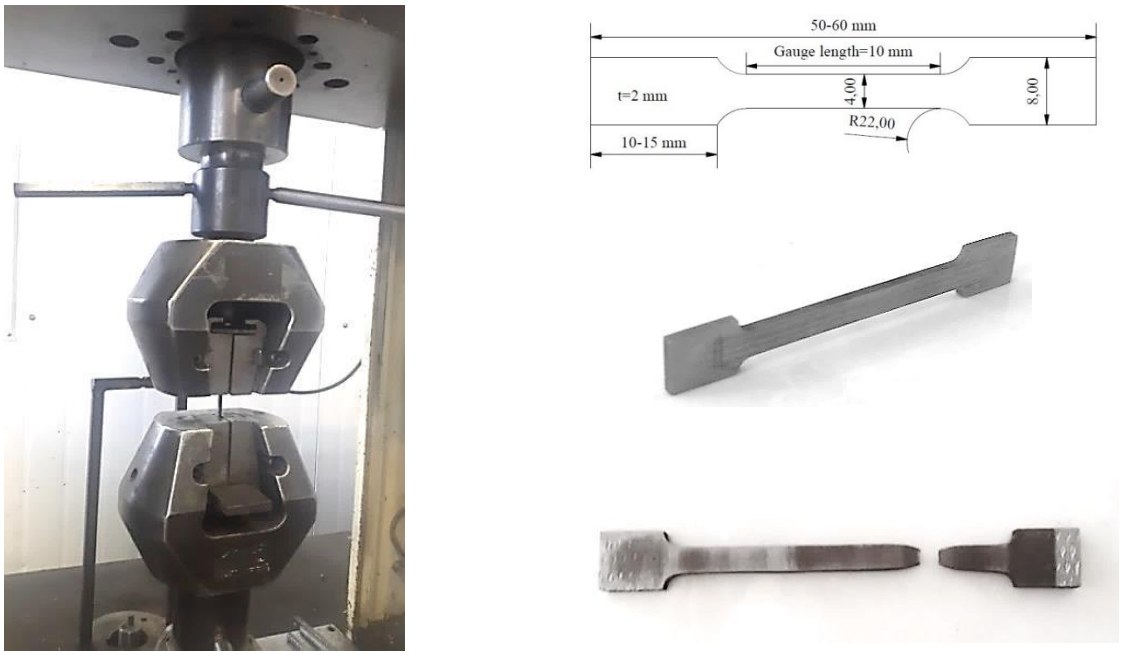

(a) **(b)**

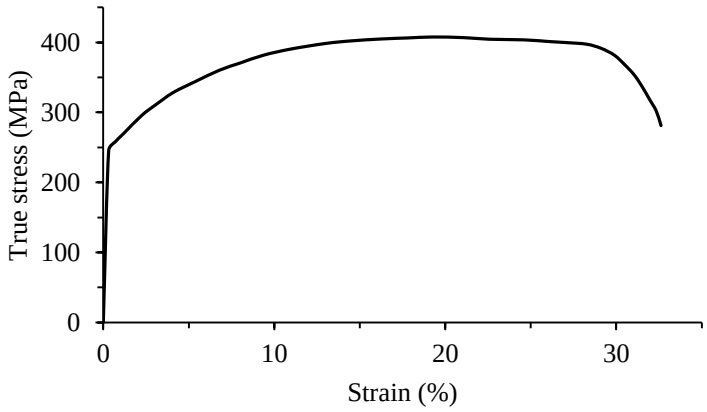

(c)

Fig. 3 Tensile test: (a) experimental setup, (b) specimens, (c) true stress-strain curve.

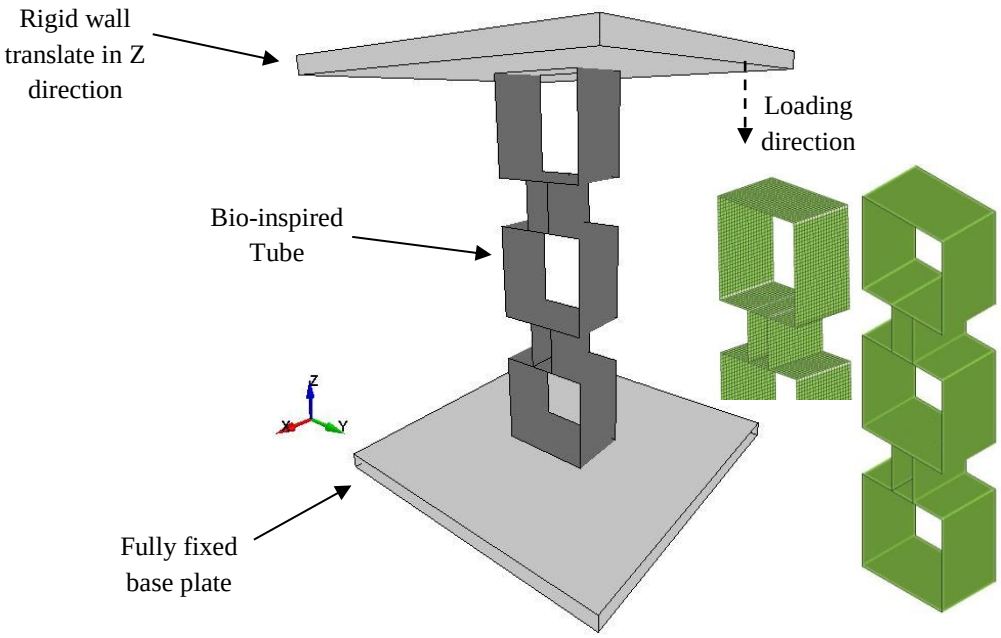

Fig. 4. Finite element model.

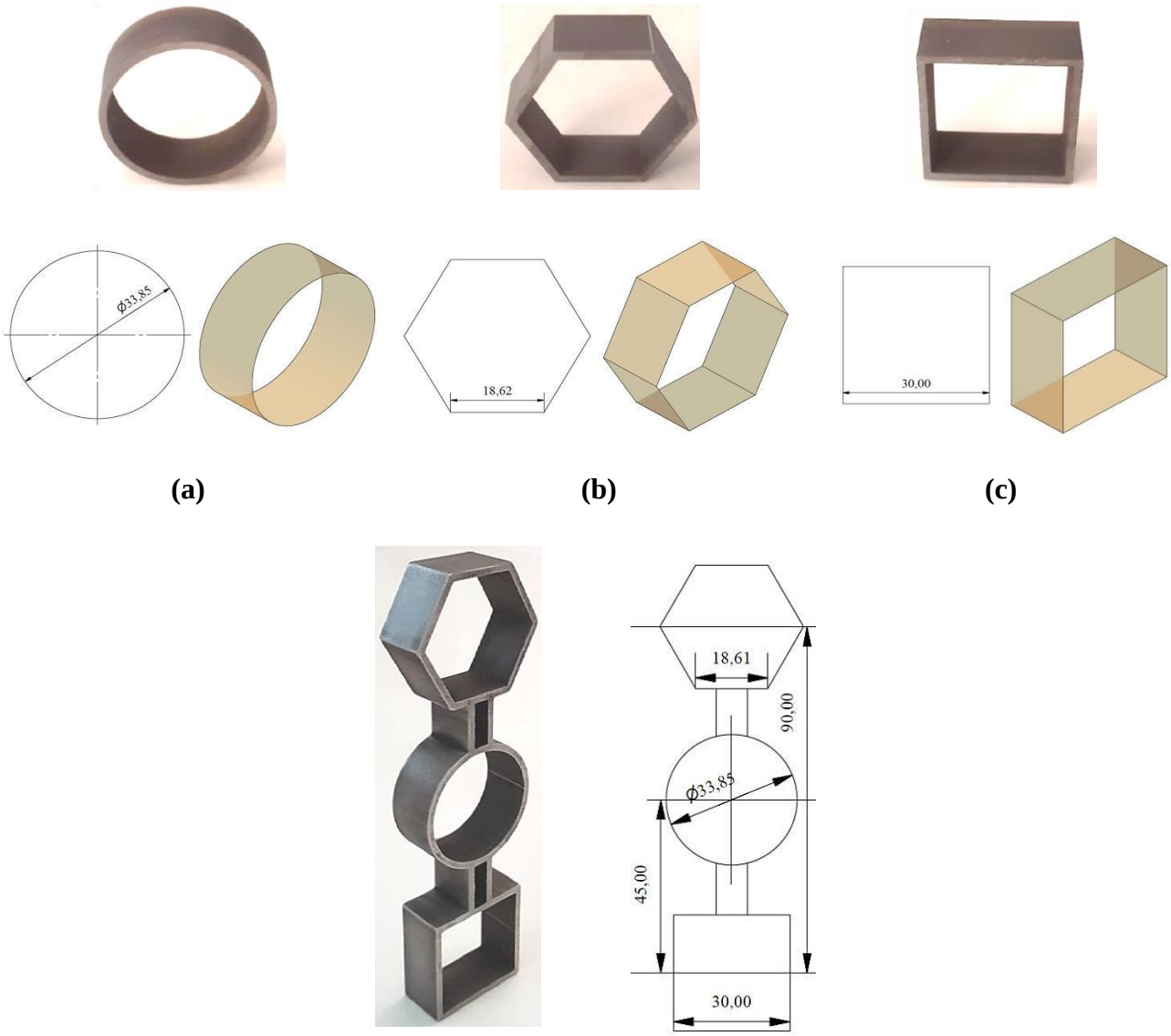

(a) **(b)** **(c)**

(d)

Fig. 5 Geometries of the tested samples: a) circular, b) hexagonal, c) square, d) H-C-S

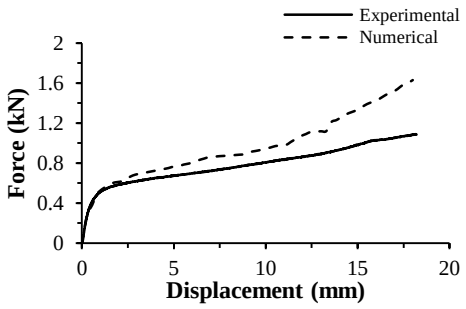
Experimental
Numerical
Force (kN)
Displacement (mm)
0
0.4
0.8
1.2
1.6
2
0
5
10
15
20

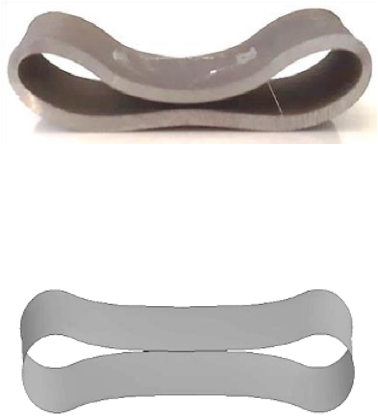

(a)

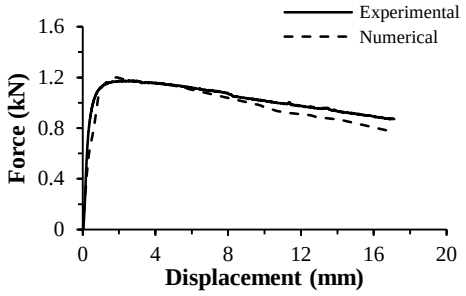
Experimental
Numerical
Force (kN)
Displacement (mm)
0
0.4
0.8
1.2
1.6
0
4
8
12
16
20

(b)

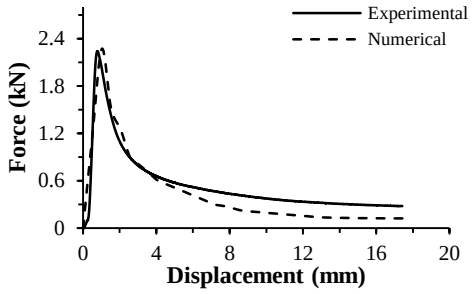
Experimental
Numerical
Force (kN)
Displacement (mm)
0
0.6
1.2
1.8
2.4
0
4
8
12
16
20

(c)

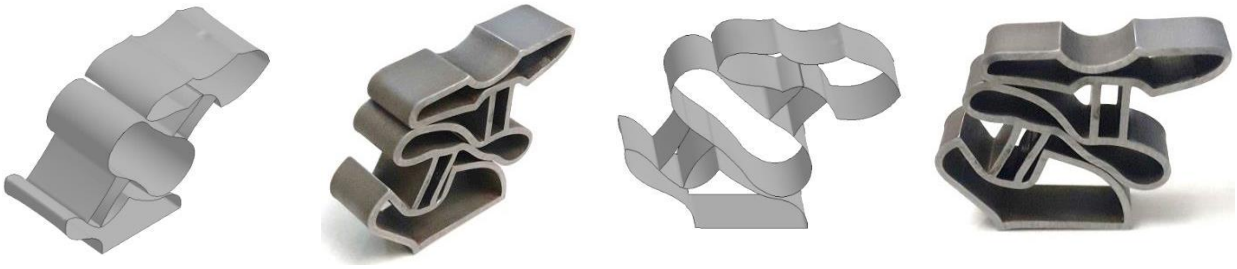

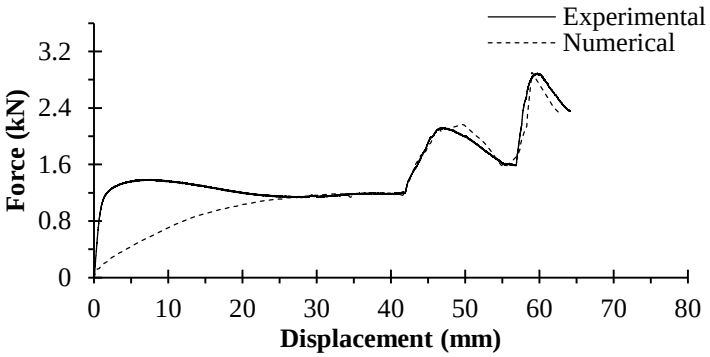

(d)

Fig 6. Experimental setup and numerical force-displacement curves and deformation mode under quasi-static lateral loading: (a) Circular, (b) Hexagonal, (c) Square, (d) H-C-S

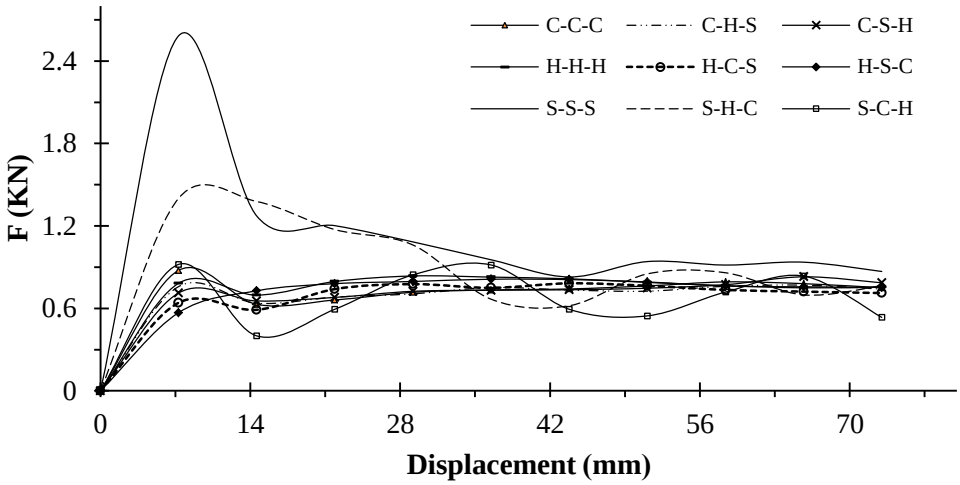

(a)

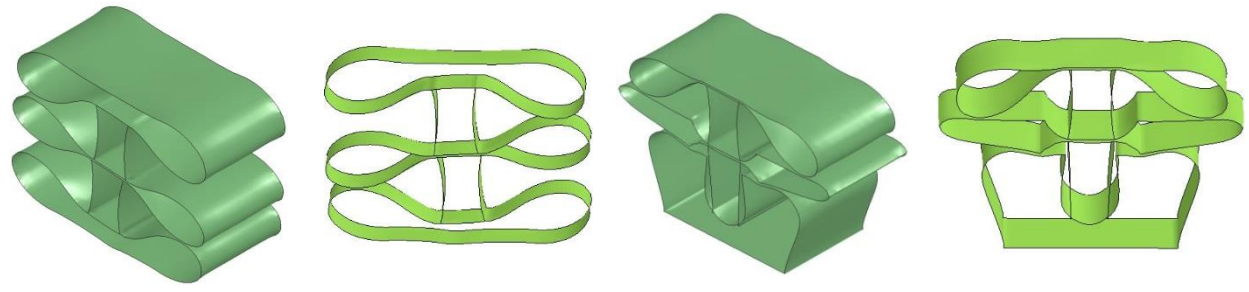

C-C-C **C-H-S**

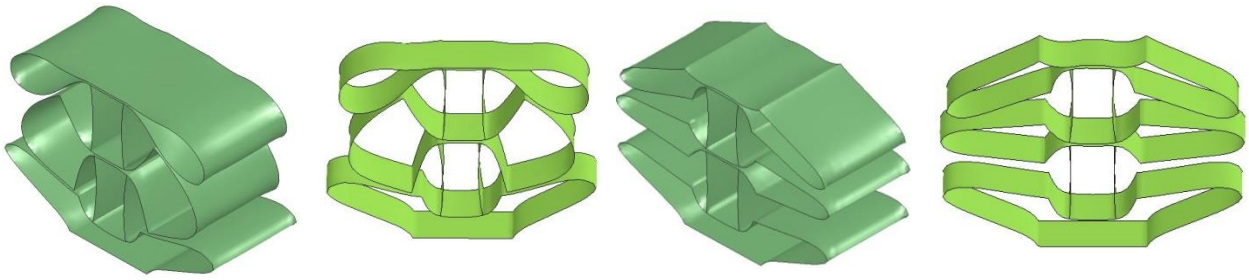

C-S-H **H-H-H**

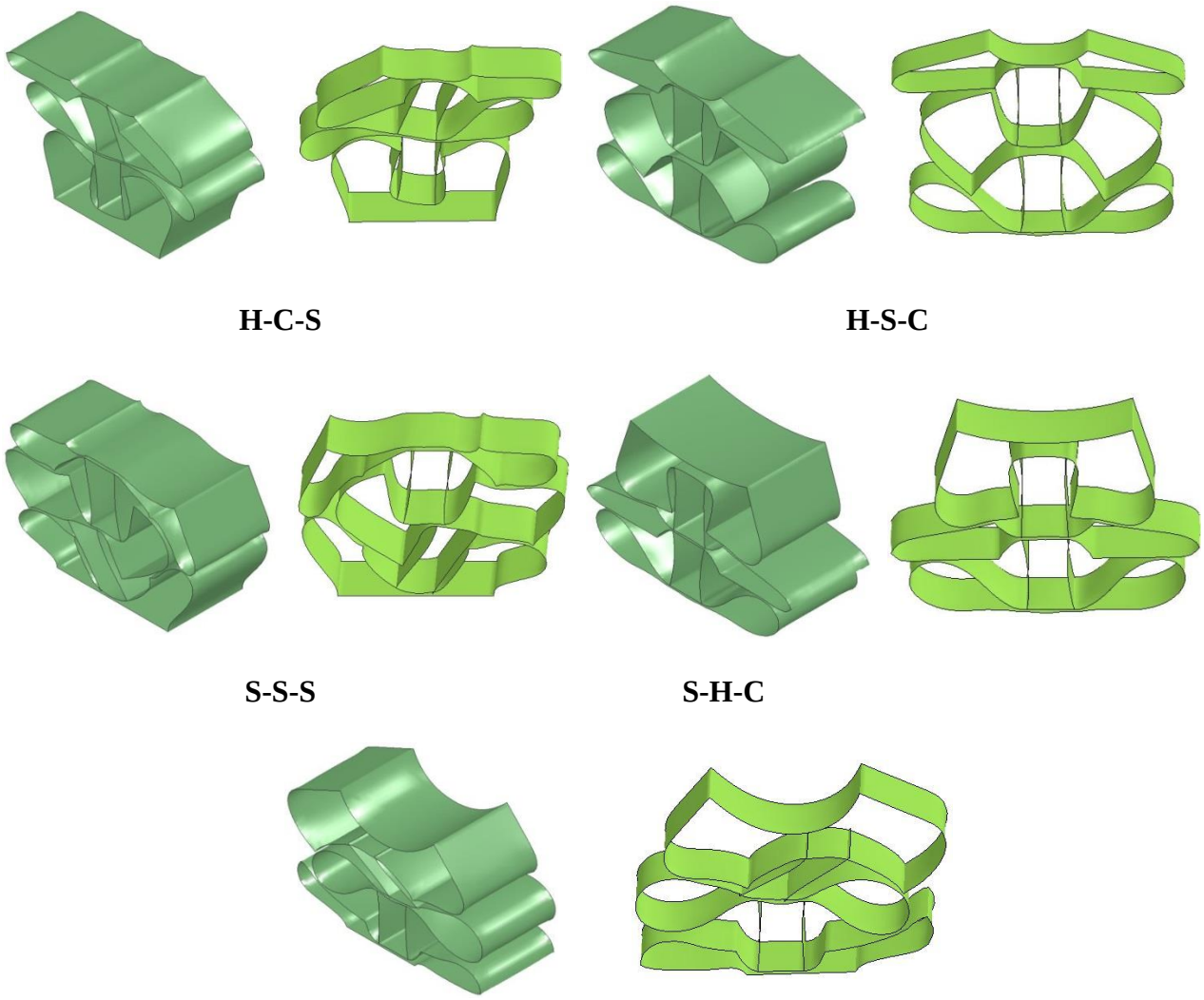

(b)

Fig. 7 a)Force-displacement curves, b) deformation modes of the bioinspired tubes with reinforcement walls

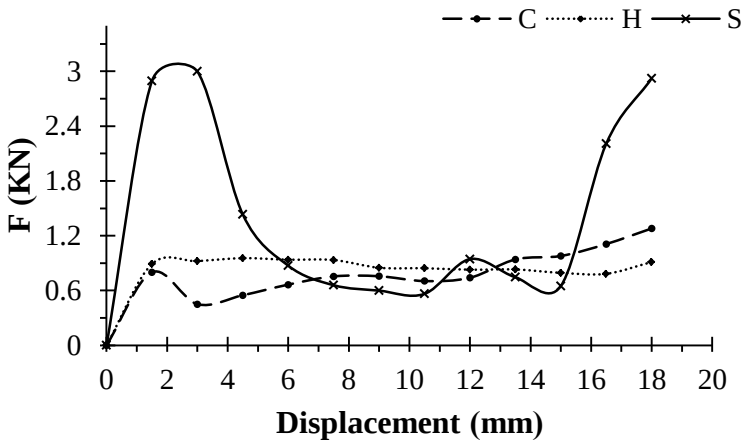
C
H
S
F (KN)
0
0.6
1.2
1.8
2.4
3
0
2
4
6
8
10
12
14
16
18
20
Displacement (mm)

(a)

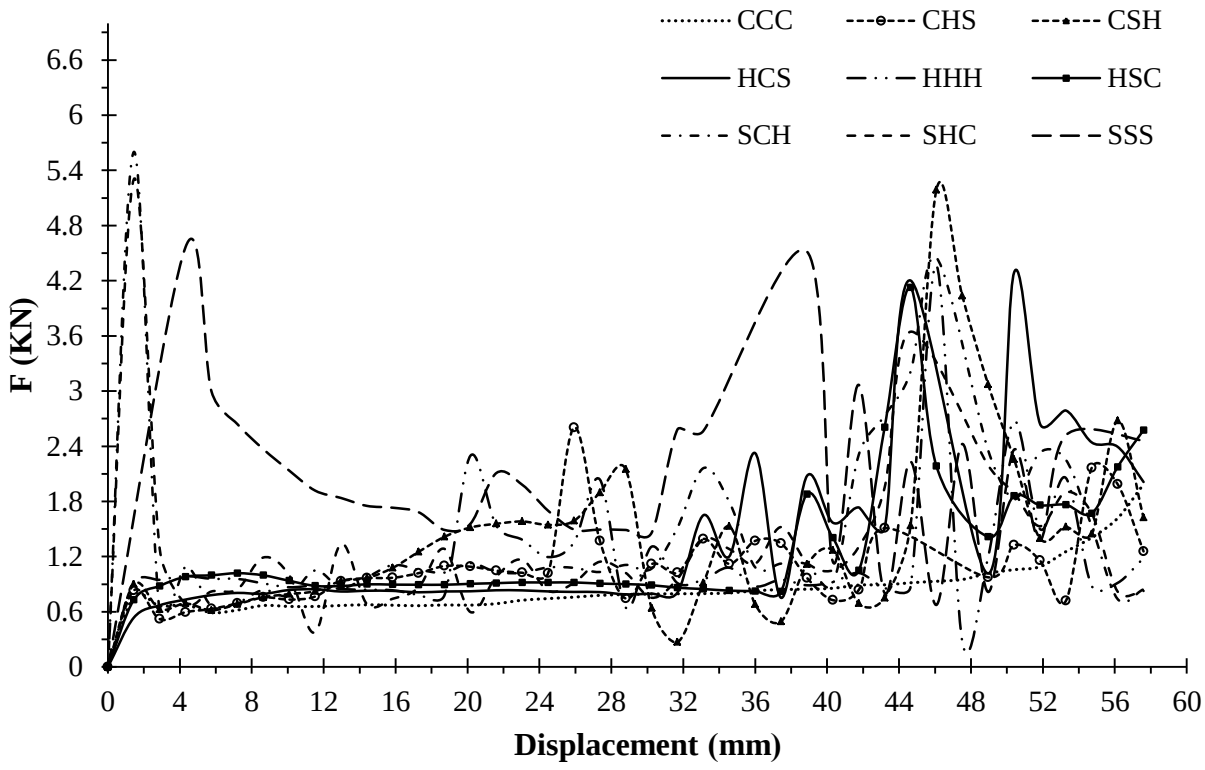
CCC
CHS
CSH
HCS
HHH
HSC
SCH
SHC
SSS
F (KN)
0
0.6
1.2
1.8
2.4
3
3.6
4.2
4.8
5.4
6
6.6
0
4
8
12
16
20
24
28
32
36
40
44
48
52
56
60
Displacement (mm)

(b)

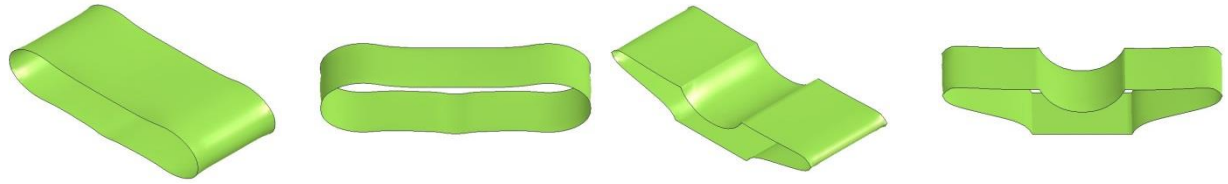

C **H**

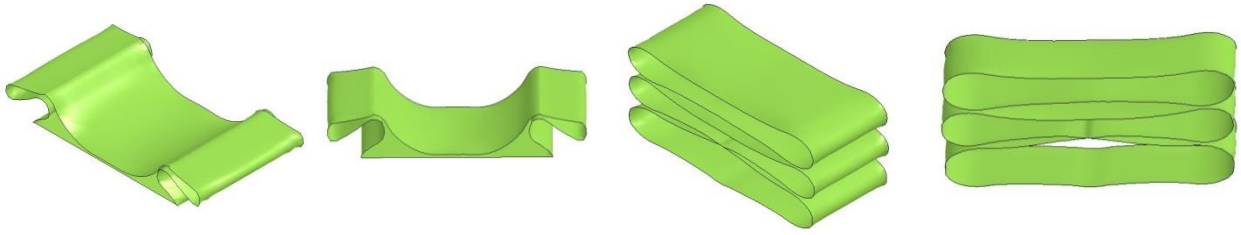

S **CCC**

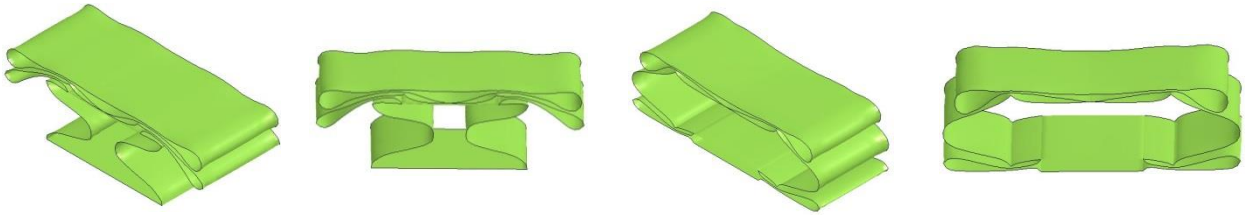

CHS **CSH**

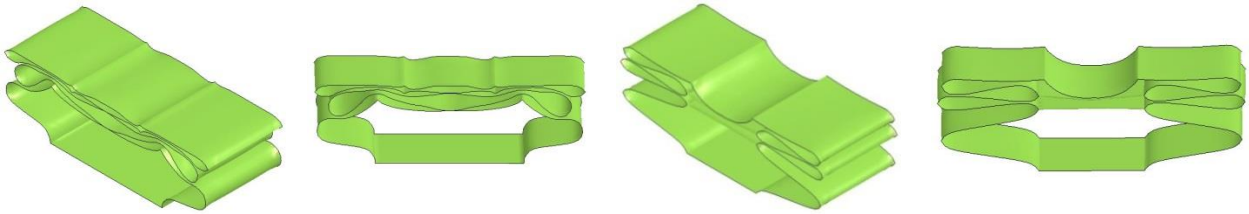

HCS **HHH**

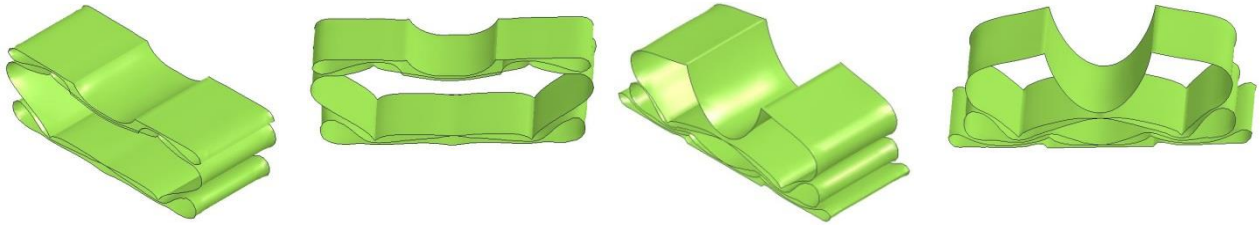

HSC **SCH**

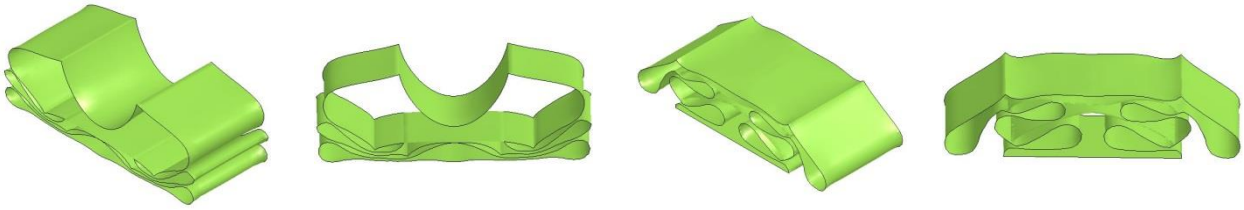

SHC **SSS**

(c)

Fig. 8 a) Traditional tubes force-displacement curves, b) Bioinspired tubes without reinforcement walls force-displacement curves, (c) deformation modes of the traditional and bioinspired tubes without reinforcement walls.

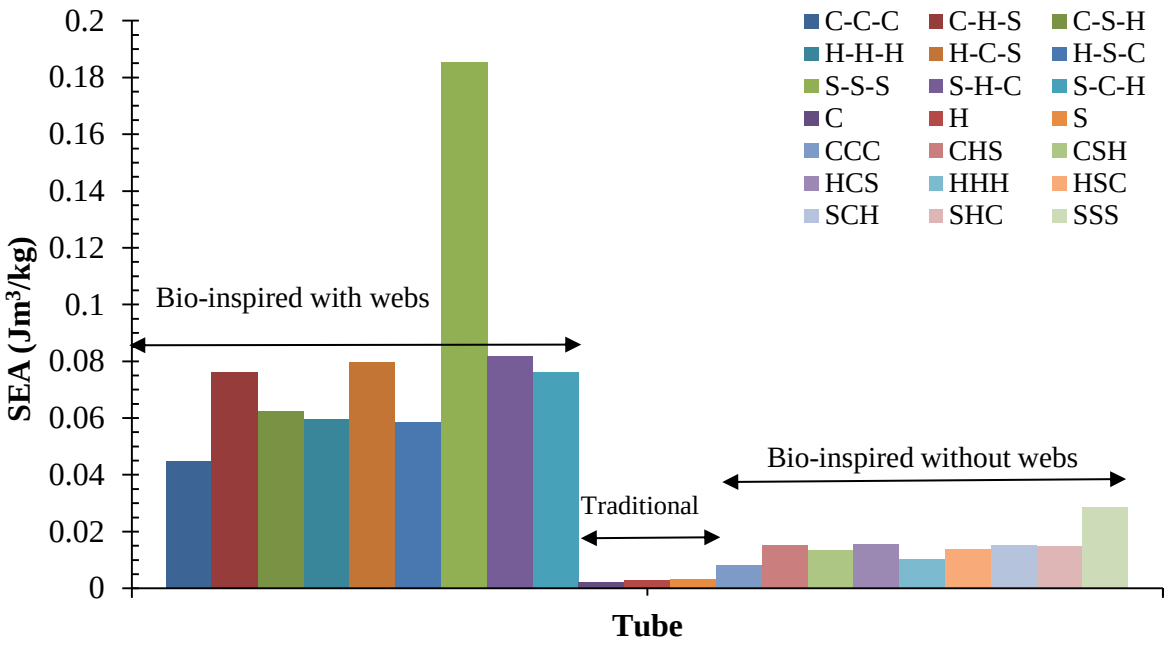
C-C-C
C-H-S
C-S-H
H-H-H
H-C-S
H-S-C
S-S-S
S-H-C
S-C-H
C
H
S
CCC
CHS
CSH
HCS
HHH
HSC
SCH
SHC
SSS
SEA (Jm³/kg)
0.2
0.18
0.16
0.14
0.12
0.1
0.08
0.06
0.04
0.02
0
Bio-inspired with webs
Traditional
Bio-inspired without webs
Tube

(a)

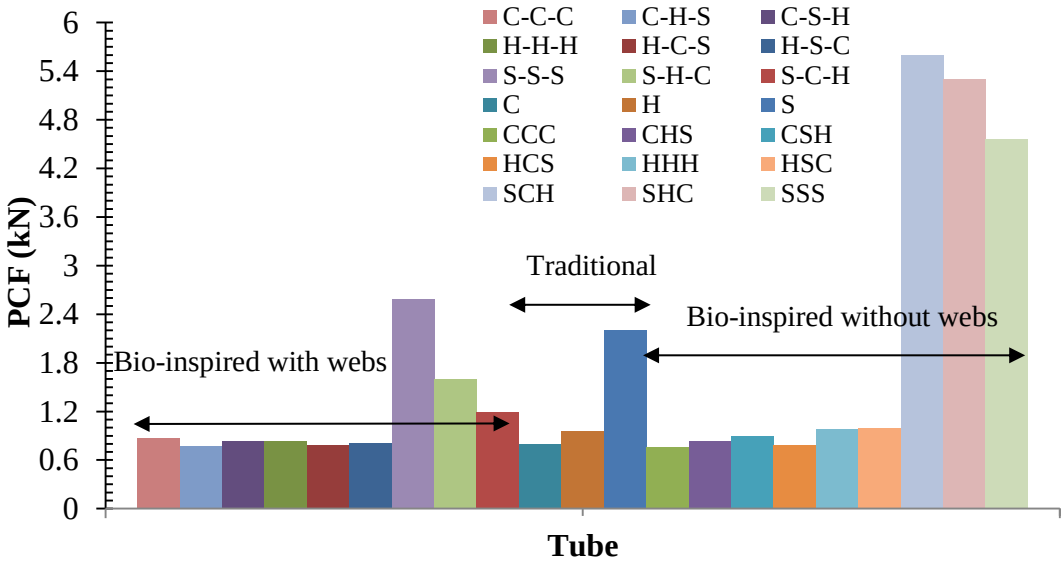
C-C-C
C-H-S
C-S-H
H-H-H
H-C-S
H-S-C
S-S-S
S-H-C
S-C-H
C
H
S
CCC
CHS
CSH
HCS
HHH
HSC
SCH
SHC
SSS
PCF (kN)
6
5.4
4.8
4.2
3.6
3
2.4
1.8
1.2
0.6
0
Traditional
Bio-inspired without webs
Bio-inspired with webs
Tube

(b)

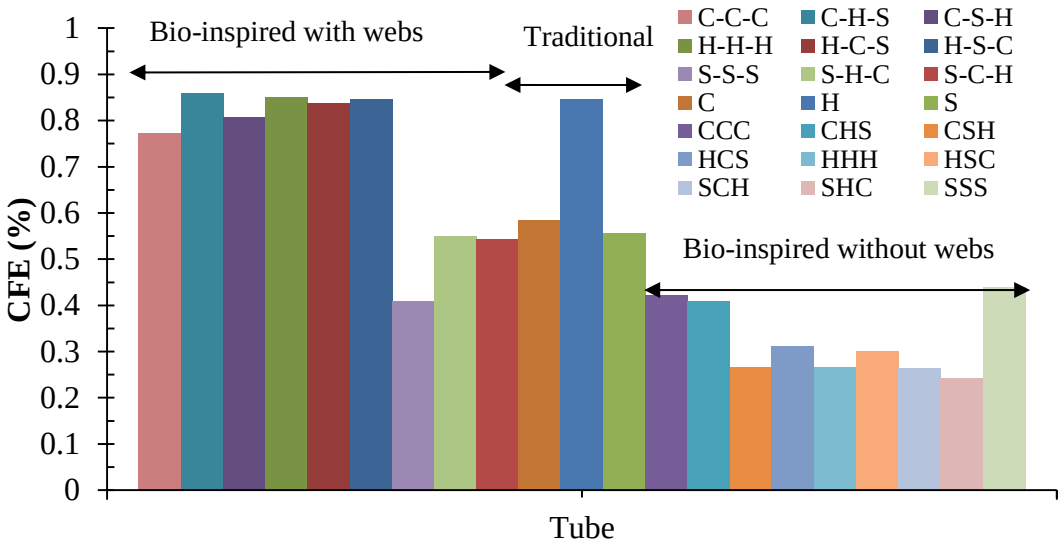

(c)

Fig. 9 Crush performance of the bioinspired tubes (a) SEA, (b) PCF, (c) CFE

Table 1. Comparison SEA, CFE, PCF of experimental tested tubes

Tube		**SEA (Jm^3/kg)**	**CFE (%)**	**PCF (kN)**
Circular	Experimental	0.0015	0.58	1.12
	Numerical	0.0022	0.68	1.63
Hexagonal	Experimental	0.0021	0.85	1.17
	Numerical	0.0019	0.81	1.20
Square	Experimental	0.0081	0.23	2.21
	Numerical	0.0074	0.19	2.27
H-C-S	Experimental	0.084	0.90	1.37
	Numerical	0.079	0.837	1.17

Table 2. Crashworthiness metrics and TOPSIS score and rank

	Crashworthiness metrics			TOPSIS	
Tube	**SEA (Jm^3/kg)**	**PCF (kN)**	**CFE (%)**	**Score**	**Rank**
C-C-C	0.044	0.876	0.772	0.0639	9
C-H-S	0.075	0.769	0.858	0.0751	3
C-S-H	0.062	0.829	0.807	0.0697	6
H-H-H	0.059	0.836	0.849	0.0693	7
H-C-S	0.079	1.17	0.837	0.0762	2
H-S-C	0.058	0.812	0.845	0.0690	8
S-S-S	0.185	2.582	0.407	0.0919	1
S-H-C	0.081	1.398	0.549	0.0701	5
S-C-H	0.076	0.998	0.544	0.0703	4
CCC	0.008	0.762	0.422	0.0528	12
CHS	0.0153	0.831	0.408	0.0534	10
CSH	0.0135	0.899	0.265	0.0515	13
HCS	0.0154	0.781	0.311	0.0529	11
HHH	0.0102	0.988	0.266	0.0504	15
HSC	0.0137	0.996	0.301	0.0512	14
SCH	0.0153	5.603	0.264	0.0041	18
SHC	0.0149	5.303	0.241	0.0057	17
SSS	0.0285	4.567	0.437	0.0219	16